Remote Sensing in Ecology and Conservation
Open Access
ZSL LET'S WORK FOR WILDLIFE

ORIGINAL RESEARCH

Spatial and temporal persistence of nearshore kelp beds on the west coast of British Columbia, Canada using satellite remote sensing

Sarah B. Schroeder[1], Leanna Boyer[2], Francis Juanes[3] & Maycira Costa[1]

[1]Spectral Lab, University of Victoria, Victoria, British Columbia V8P 5C2, Canada
[2]SeaChange Marine Conservation Society, Brentwood Bay, British Columbia V8M 1R3, Canada
[3]Department of Biology, University of Victoria, Victoria, British Columbia V8P 5C2, Canada

Keywords
Bull kelp, change analysis, coastal regions, nearshore habitat, remote sensing, satellite

Correspondence
Sarah B. Schroeder, Spectral Lab, University of Victoria, Victoria, B.C. V8P 5C2, Canada.
Tel: 250-4725223; Fax: 250-721-6216;
E-mail: sbs@uvic.ca

Editor: Kate He
Associate Editor: Vincent Lecours

Received: 19 August 2019; Revised: 21 November 2019; Accepted: 22 November 2019

doi: 10.1002/rse2.142

Remote Sensing in Ecology and Conservation 2020;**6** (3):327–343

Abstract

Bull kelp *Nereocystis luetkeana* is an important foundation species, providing structural habitat and nutrients to the nearshore ecosystems of temperate coastal regions in the Northeast Pacific. Sensitive to environmental conditions, this species thrives in cool, nutrient-rich water. Reported declines in the extent and distribution of bull kelp may reflect changing oceanic conditions and result in breakdown of important food chains and ecosystem services. This study uses satellite remote sensing to map kelp bed extent from 2004 to 2017 in the Salish Sea on the West Coast of British Columbia, Canada and examines the relationship between trends in kelp persistence with local and global scale environmental conditions. In our study area, we found limited evidence of kelp decline. Local scale effects of current speed, temperature and substrate type may play a role in the spatial and temporal patterns of persistence. Kelp persistence was higher in sites with rocky substrate and lower in areas with low current and gravel or sand substrate. A decline in kelp was recorded from a high in 2015 to a low in 2017; however, a longer and more complete record is needed to distinguish declining trends from natural variability. This work highlights the importance of continued collection of long-term data for use in time series of kelp abundance as multiple factors can influence the reliability of image interpretation and kelp classification.

Introduction

As one of the most productive ecosystems on the planet (Steneck et al. 2002; Krumhansl and Scheibling 2012), kelp forests support high biodiversity, providing protection, habitat and foraging opportunities for invertebrates, fish, birds and mammals (Estes et al. 1989; Christie et al. 2009), and as such are an important indicator of ecosystem health (Claisse et al. 2012; Uhl et al. 2016). Furthermore, the physical structure of kelp beds influence coastlines through dampening of waves and providing nutrient subsidies to shorelines as wrack (Teagle et al. 2017).

Globally, kelp species are found growing on rocky reefs in temperate coastal regions, in response to abiotic drivers: temperature, nutrient, photosynthetically active radiation (PAR), substrate type, current and wave stress (Cavanaugh et al. 2011), and biotic: grazing and competition (Duggins 1980). Optimum growth conditions happen in cool nutrient-rich waters, associated with temperate coastal regions; however, prolonged periods of warmer than average temperatures (>17°C) reduce spore production and cause kelp die-off (Vadas 1972; Schiel et al. 2004). Beyond increased ocean temperatures, other stressors including increased storm frequency, direct harvest and the effects of overfishing contribute to collapse of kelp ecosystems (Halpern et al. 2006; Lorentsen et al. 2010; Hernández et al. 2018). The degree to which these stressors influence kelp varies, with regional differences playing a key role and an overall downward trend of abundance worldwide (Krumhansl et al. 2016).

Specifically, run-off associated with anthropogenic activities such as agriculture and forestry increases sediment loads in river effluent and has strong negative

impacts on kelp beds through the reduction of PAR and smothering of recruits (Shaffer and Parks 1994; Carney 2005). Disturbance caused by wave and current can also have large impacts on the abundance of kelp, where areas of low current may leave kelp more susceptible to herbivory and high current or wave exposure may limit growth due to physical removal (Reed et al. 2011). In regions where predators such as sea otters or predatory fish have been removed through over-fishing, herbivores such as urchins thrive and have significant impacts on kelp bed size and abundance through unchecked grazing (Steneck et al. 2002; Foster and Schiel 2010). Additionally, changes in environmental conditions, which are unfavorable for kelp growth, may give rise to dominance by other species, such as coralline and turf algae resulting in a shift to altered stable states (Filbee-Dexter and Wernberg 2018). Increased herbivory and warmer ocean temperatures can combine to cause major declines in kelp forest abundance (California Department of Fish and Wildlife, 2016; Burt et al. 2018).

These different kelp stressors have been reported for several regions of the world. In the Salish Sea, on the West Coast of North America, one of the dominant canopy-forming kelps, bull kelp (*Nereocystis luetkeana*) (Druehl 1968) has shown variability in abundance with most declines recorded in regions adjacent to dense urban areas (Pfister et al. 2018). Fluctuation in abundance has also been linked to both broad scale oceanic conditions such as the Pacific Decadal Oscillation and North Pacific Gyre Oscillation, and to local scale impacts on water quality, temperature and increased herbivory (Taylor and Schiel 2005; Foster and Schiel 2010; Burt et al. 2018; Pfister et al. 2018).

Differences between global and local scale changes in kelp abundance may reflect regionally dependant influences where the local effects of grazing pressure, water quality and possible resilient populations interact with large-scale environmental fluctuations, which result in decline, reduced resilience or alternative stable states depending on the combination of factors (Krumhansl and Scheibling 2012). Understanding the drivers, their outcomes and effects on associated ecosystems requires both long-term and large-scale maps of kelp abundance. Mapping kelp extent has been a requirement for conservation and monitoring initiatives including quality of salmon habitat (Shaffer 2004), creation of marine protected areas (Airamé et al. 2003), regulating harvest impacts (Sutherland et al. 2008), oil spill impact monitoring (Peterson et al. 2003) and climate change adaptation services programs (Duarte et al. 2013).

Satellite imagery has been successfully used to map spatial-temporal changes in canopy kelp (Deysher 1993; Stekoll et al. 2006; Young et al. 2016). Many of these successful analyses focus on species that form large beds, such as giant kelp, *Macrocystis pyrifera,* allowing the use of lower spatial resolution imagery from Landsat (Cavanaugh et al. 2010). However, detecting bull kelp, which may form fringing beds adjacent to the shoreline, may require high spatial resolution satellite, aerial or drone images ranging from 0.2 m to 2–4 m in resolution (Deysher 1993; Schroeder et al. 2019). This study uses a time series of high-resolution satellite imagery from 2004 to 2017 to map bull kelp beds on the West Coast of British Columbia, Canada, and provides an analysis of changes in kelp persistence and its relationship to global and local scale environmental conditions.

Materials and Methods

Study area

The study area covers approximately 50 km of coastline in Cowichan Bay and Sansum Narrows, located in the Salish Sea on the West Coast of British Columbia, Canada (Fig. 1). Tides in this semi-enclosed body of water are mixed semi-diurnal with exchange of water from the open ocean through the Straits of Georgia and Juan de Fuca. Freshwater inputs come from the Cowichan and Koksilah Rivers directly into Cowichan Bay (450 m^3 s^{-1} during peak flow in winter) as well as input from the Fraser River to the east (10 000 m^3 s^{-1} during spring freshet). In summer, warm ocean temperature and peak flow from the Fraser River create stratification in the water column in the Strait of Georgia, which leads to increased surface water temperature (14–21°C) and decreased salinity (26–28 PSU) (Waldichuk 1957; Chappell and Pawlowicz 2018). However, water flowing through the Southern Gulf Islands with localized regions of high currents due to the narrow channels between the islands, tends to have increased mixing than that in the Strait of Georgia, resulting in slightly lower temperatures and higher salinity (Waldichuk 1957).

The coastline in this region consists of rocky cliffs, mixed gravel beaches, sand and mudflats on which several species of aquatic vegetation grow. These habitats support a number of commercially and ecologically important species including Chinook *Oncorhynchus tshawytscha* and Coho *Oncorhynchus kisutch* salmon, whose populations have declined precipitously in recent years and for whom loss of habitat including kelp may be a contributing factor (Waldichuk 1957).

Imagery database

A time series of high-resolution imagery from 2004 to 2017 were selected from the Digital Globe archives considering the preliminary criteria: spatial resolution of

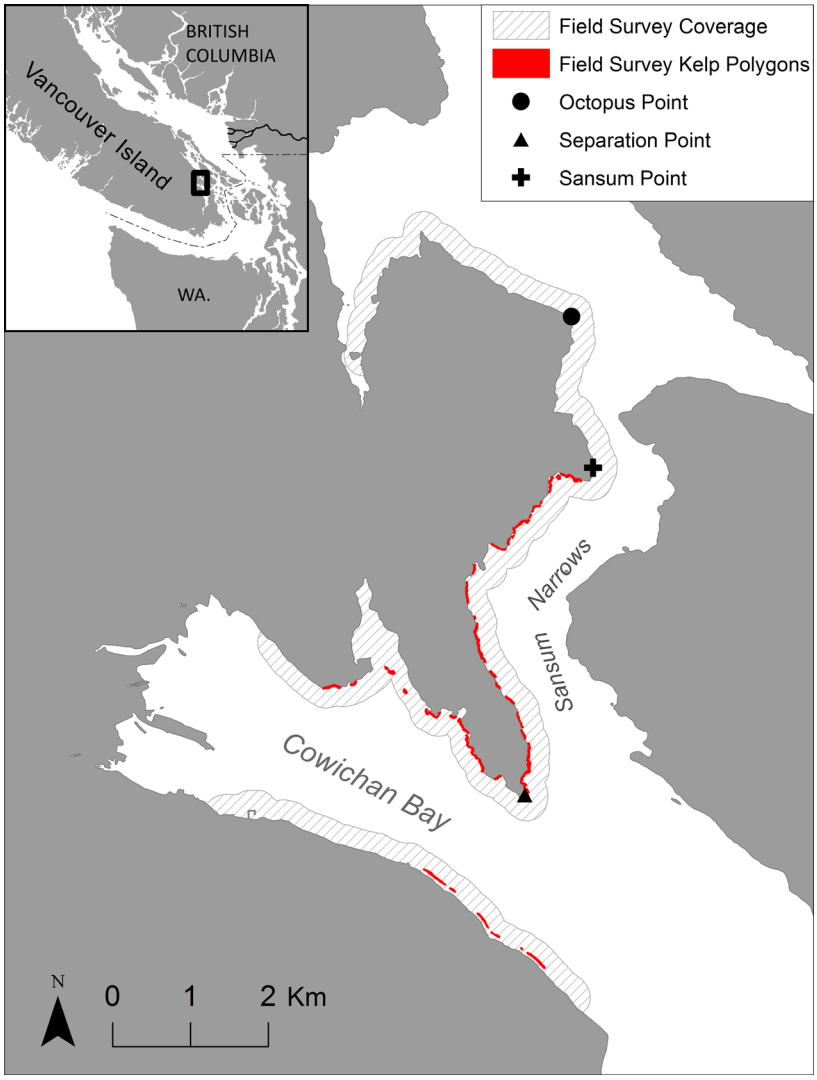

Figure 1. Study area including Cowichan Bay and Sansum Narrows on the East Coast of Vancouver Island, British Columbia, Canada. Red polygons are kelp beds delineated by a kayak-based field survey in August 2016. Hatched lines indicate the total area covered by the kayak-based field survey in August 2016.

2.5 m or higher, spectral resolution containing visible and near infrared (NIR) bands, minimal clouds and acquisition during peak kelp growth in summer. This selection resulted in eight images (Table 1). From these images, further criteria were developed to determine the reliability of the images for accurately mapping kelp. Similar to the methods by Nahirnick et al. (2019), each image was scored from 1 to 3 with one being the poorest condition, according to the following criteria: (1) time of collection within the growing season; (2) tide height, where lower tides allow for better ability to detect kelp floating on the water surface; (3) intensity of glint on the water, where high glint obstructs the ability to detect kelp; (4) water surface roughness (WSR), which describes the texture of the water surface, where calm flat water is best for detecting kelp and breaking waves or white caps present difficult conditions (Table 2). The total score (maximum of 12) for each image was calculated and images with scores lower than seven were deemed too unreliable for kelp detection. Due to constraints in the overlap among all images, only five of the seven images meeting the quality criteria were used for further analysis (Table 1). This method resulted in selected images acquired in 2004, 2012, 2015, 2016 (tasked with concurrent field data), and 2017. Finally, the scores from the images which qualified for analysis were used to assess whether image quality played a role in the resulting kelp maps.

In situ dataset

The *in situ* data set comprised of a kelp survey and above-water reflectance data acquisition. Field data acquisition was conducted during the time of the 2016 image acquisition using kayak and GPS methods following

Table 1. Quality parameters for all images in database.

Sensor	Spatial resolution	Year	Date	Tide height	Glint	WSR	Score
QB	2.6 m	2004	Sept 24th	1.8 m	None	Minimal	10
WV2	1.8 m	2012	July 29th	1.5 m	Medium	Medium	9
WV2	1.8 m	2015	August 27th	1.2 m	Minimal	Minimal	12
WV3	1.2 m	2016	August 30th	1.2 m	Medium	Medium	10
WV3	1.2 m	2017	July 27th	1.5 m	Minimal	Minimal	11

Sensors are QB = QuickBird series, WV = WorldView series.
WSR, Water surface roughness.

Fretwell & Boyer, (2010) covering North and South Cowichan Bay and West Sansum Narrows to Maple Bay (Fig. 1). Three teams of experienced mappers and volunteers with hand-held GPSs paddled along the shoreline during the mapping window of one hour before and after low slack tide (1.1 m). All canopy kelp floating on the water's surface was recorded as either a single bulb, multiple bulbs, line of kelp or a bed. The GPS points were digitized and used to create kelp polygons in ArcGIS for use as data in validation of classification methods. Possible uncertainties associated with this field data are: (1) error in the GPS units, which recorded accuracy between 1 and 9 m, (2) errors in the kayakers' ability whereby points may not be exact due to the nature of collecting data in a moving platform with currents, waves and in close proximity to rocky outcrops, and (3) changes in the location of kelp between the time of the field survey and the acquisition of the image due to differences in tide height and current speed. Due to these issues, a 10 m uncertainty buffer was added around the field-derived kelp polygons, and points extracted for use in training or validation of classification were not collected in this buffer.

Above-water *in situ* kelp and water spectra were collected in the field to record the spectral characteristics of different combinations of kelp and water for further analysis of the classification results. A calibrated hand-held FieldSpec® spectroradiometer with a spectral range from 325 to 1075 nm was used to collect spectra of various densities of floating kelp, deep water and kelp submerged within approximately 20 cm of the water surface in August 2017. A sample number of n = 10 was collected for each kelp-water combination of dense, sparse, submerged kelp and pure water under conditions of clear sky and calm water. Spectral measurements were acquired by boat within and beside kelp beds in the study area with a sensor viewing geometry of 1 m from the water's surface, held at a 45° angle zenith, and 90° azimuth to incoming solar radiation to prevent specular reflection (Adler-Golden et al. 1999). Reflectance measurements were averaged, and four classes were defined as dense (>50% of the sensors field of view (FOV) covered with kelp), sparse (<50% of FOV), submerged and pure water (Fig. 2). The spectral signature of kelp shows high reflectance in the near-infrared (NIR) and low reflectance in red bands, while sparse or submerged kelp beds show lower ratio of NIR to red due to the effect of water, which strongly absorbs NIR (detailed spectral analysis in (Schroeder et al. 2019)).

Image processing

Image processing methods included geometric, radiometric and atmospheric correction, masking, image enhancement, transformation and classification. First, historical images were georectified using the 2016 geometrically corrected image as reference, resulting in root mean square errors of less than 0.06 m. Next, images were radiometrically corrected and atmospherically corrected (Adler-Golden et al. 1999) using the FLAASH module in ENVI v5.5, to minimize atmospheric effects and convert radiance signal to surface reflectance. To ensure that the reflectance values were comparable to the 2016 base image, all historical images were normalized using

Table 2. Image reliability scoring metrics

Score	Season	Tide height	Glint	WSR
Ideal (3)	Late July to early September	≤1.2 m	No glint	Smooth calm water
Medium (2)	Mid-June to late July or mid-September to late September	1.3–2 m	Some glint	Some surface texture
Poor (1)	Before mid-June or after September	>2	High glint throughout image	Breaking waves

WSR, water surface roughness.

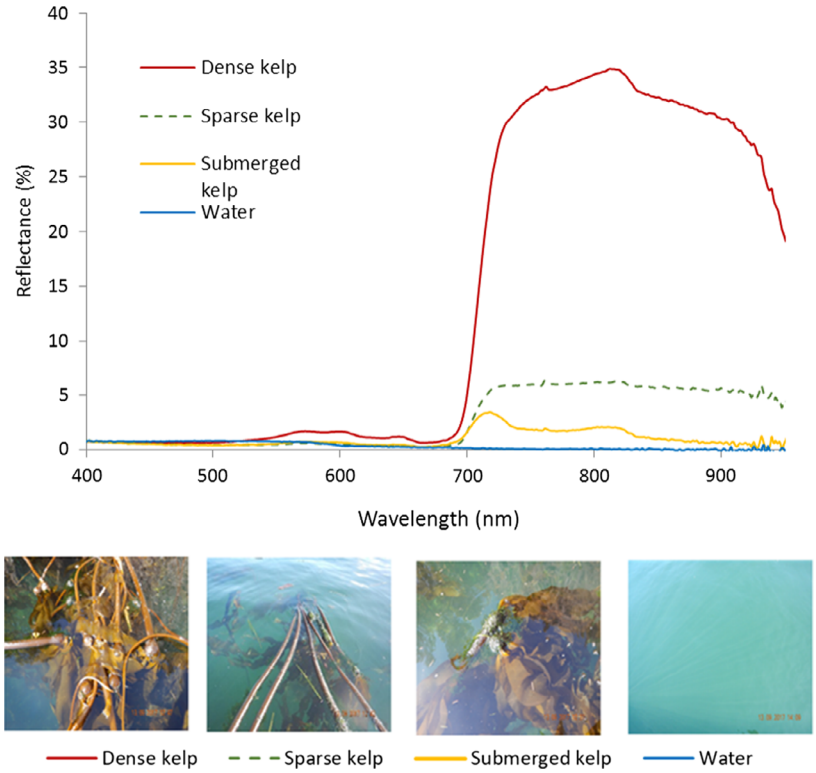

Figure 2. Representative reflectance of dense (>50% of FOV), sparse (<50% of FOV), submerged kelp and ocean water measured with a Fieldspec Pro® spectroradiometer in the coastal waters of British Columbia, Canada (source: Schroeder et al. 2019).

pseudo invariant features with the 2016 image as reference (Fig. 3). This procedure allows for reflectance spectra of features of interest to be comparable for the different years, and therefore improving the performance of the classification results (Bao et al. 2012). Despite these corrections, water reflectance varied slightly from year-to-year likely due to differences in characteristics of optical constituents in the water (Fig. 3). This variability will be reflected in the spectral response of any image pixels containing kelp as the reflectance of each pixel is a product of the ratio of kelp and water as established in Figure 2.

Following normalization, a land mask was created for each image, using object-based image segmentation with Definiens eCognition® using the NIR (band 4), Red (band 3) and Green (band 2) bands as input to accentuate the contrast between the high reflectance of terrestrial vegetation and rocky shoreline compared to the low reflectance of water along the shoreline. A 4 m buffer was added to the resulting land mask to eliminate adjacency effects from terrestrial vegetation and the presence of other nearshore algae such as *Fucus* spp. and *Ulva* spp. This masking method allowed precise delineation of the shoreline at the slightly different tide levels present between images. Next, a deep-water mask was applied using the 30 m isobaths created using multibeam data acquired from the Canadian Hydrographic Service. This represents the maximum depth at which kelp generally grows in this region (Springer et al. 2007).

After applying the unique masks to each image, the reflectance-based products were defined for optimizing input to the classification. A series of possible indices, reflectance transformations and reflectance bands were tested for effectiveness in separating kelp from other cover types using the 2016 image and a subset of the field survey data. Using the Jefferies-Matusita distance statistical metric (Padma and Sanjeevi 2014), NDVI (Eq.1) and GNDVI (Eq.2) were defined as best able to separate kelp from water, glint, shallow substrate and terrestrial vegetation in shadow. NDVI is the normalized difference vegetation index developed to enhance the detection of vegetation (Rouse et al. 1974) and is applicable to bull kelp due to kelp's similar reflectance properties (Fig. 2); GNDVI or the green normalized vegetation index uses the green wavelengths instead of red, and is more sensitive to chlorophyll concentrations than NDVI (Goldberg et al. 2016).

$$\mathrm{NDVI} = \frac{\mathrm{NIR} - \mathrm{Red}}{\mathrm{NIR} + \mathrm{Red}} \quad (1)$$

$$\mathrm{GNDVI} = \frac{(\mathrm{NIR} - \mathrm{Green})}{(\mathrm{NIR} + \mathrm{Green})} \quad (2)$$

Additionally, a principal component analysis (Gupta et al. 2013) showed that PC1 was advantageous because

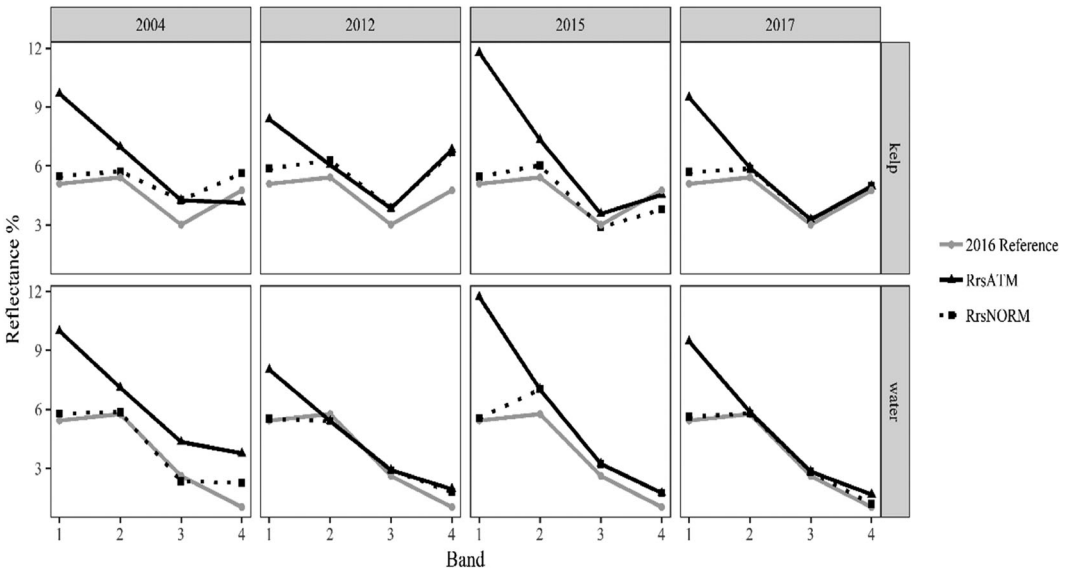

Figure 3. Example of normalization for water based on the 2016 corrected image (2016 Reference), and results before (RrsATM) and after normalization (RrsNorm) for each image year. Note the generalized decreased reflectance in band 1 (blue spectra) between RrsATM and RrsNORM showing improved Rayleigh correction, and the expected low and high band 4 (NIR) reflectance for water and kelp, respectively.

of its ability to separate kelp from shadow over water that was not previously masked due to its similar reflectance to kelp. These indices and transformations were combined as input for classification.

Classification

The unsupervised ISODATA classification method (Tou and Gonzalez 1974) was deemed reliable for classification of historical imagery as it can be used without field survey data, which was only available for 2016. This method was tested against several classification methods using the 2016 image and concurrent field survey data, and the results showed that the ISODATA approach performed similarly to supervised methods (Young et al. 2016).

The ISODATA classification produced several classes for each image (8–12) and reflectance spectra for each class were compared to the known spectra for dense and sparse kelp derived from the 2016 image and *in situ* above-water spectra. These relationships were used to determine which of the defined classes should be categorized as kelp and then statistically confirmed in the validation step (Fig. 4, Table 4). Finally, a filter to remove single isolated pixels identified as kelp that were separated by greater than eight pixels was applied; this situation may happen due to glint.

After the classification, the resulting kelp maps were validated following two distinct procedures due to availability of *in situ* data: (1) 2016 image, accuracy assessment based on concurrent *in situ* samples and (2) for the other years without concurrent field data, a statistical approach was taken. For the 2016 image, a confusion matrix was constructed using 849 randomly selected samples from the field data for accuracy assessment, and an error matrix was constructed to determine users, producers and total accuracy. For the remaining images (2004, 2012, 2015, 2017), accuracy assessment was accomplished using the non-parametric Wilcoxon signed-rank test (Taheri and Hesamian 2013) to determine whether pixels classified as kelp in both, 2016 reference image versus historical image, were spectrally statistically similar. First, a random sample of pixels (n = 500) from the classification results was collected for each image and the spectral information from NDVI and GNDVI were extracted. PC1 values were not compared, as they are a function of the data within a scene and not expected to remain similar between images (Schowengerdt 2012). The analysis takes into consideration that the output ranges of NDVI and GNDVI are a function of the proportion of highly reflective kelp in the NIR to highly absorbing water within each pixel.

Change analysis

Several factors affect the accuracy of measuring changes in kelp extent derived using satellite-based methods, including:

1 Differences in the kelp extent in a given area from year-to-year. This may be caused by the dynamics of

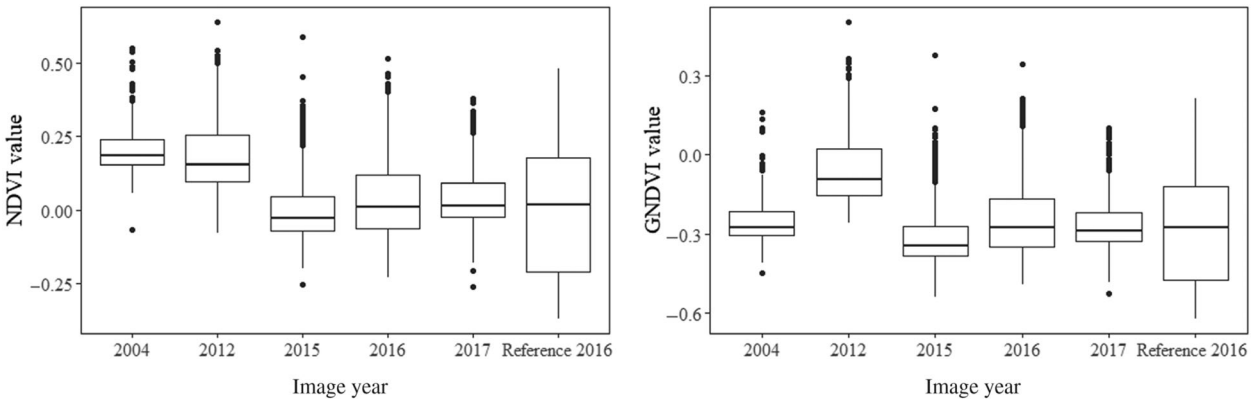

Figure 4. Boxplots of the relative distributions of sampled kelp pixels (n = 500), for the classification results of 500), for the classification results of each image year and the reference.

the environment during the growing season including temperature, nutrients, PAR and biotic interactions (Springer et al. 2007), as well as growing conditions in the previous year or years affecting the production and viability and settlement of spores (Cavanaugh et al. 2011; Pfister et al. 2018). This would be considered a true change in kelp extent.

2 Differences in the timing of peak kelp growth due to growing conditions from year-to-year. As bull kelp is an annual species, the timing of peak kelp growth may have natural variability from year to year depending on the growing conditions, including temperature, nutrient and light availability (Springer et al. 2007). Extended periods of warm surface waters may also cause early die off in populations where peak growth is usually in late summer (Mumford 2007; Simonson et al. 2015). In this case, images collected prior to or after peak growth may underestimate maximum kelp extent.

3 Differences in image quality due to environmental conditions at the time of acquisition including tide height, glint and water surface (Schroeder et al. 2019). Effects of currents can cause changes to surface kelp extent on an hourly and even minutely basis (Britton-Simmons et al. 2008). In this case, maximum kelp extent is present but is obscured by waves, glint or water column and is not detected in the image.

Together, these factors add complexity and uncertainty on how to define change in kelp extent based on area derived from image pixels. Satellite images offer a "snapshot" of kelp extent, which may only represent a portion of the total kelp present in a given season depending on the conditions explained above. To overcome this problem, we adopted a method similar to that used in Pfister et al. (2018) in which shoreline units were used to analyze changes in kelp. We divided the study area into 100 m bins (shoreline units) taking into consideration the characteristics of the region, including the exposure, orientation and the average size of kelp beds data from the British Columbia Marine Conservation Analysis (BCMCA) (British Columbia Marine Conservation Analysis Project Team, 2011), *in situ* observation and field data. Within each bin, the number of times kelp was mapped over all the images was defined and expressed as a kelp persistence measure. For instance, a persistence of 100% indicates that kelp was present in a bin in all years analyzed. Note that due to the limited spatial coverage of the 2004 image, the east side of Sansum Narrows (Fig. 5) was analyzed separately using the remaining four images (2012, 2015, 2016, and 2017); for this area, 100% persistence equals to kelp present in 4 years. Drivers of spatial and temporal kelp persistence were considered based on known factors that influence kelp growth and reproduction and data availability. High-resolution data of substrate and current strength allowed sub regional variation to be explored whereas sea surface temperature and climate indices were considered at a regional scale. Substrate type was identified through the ShoreZone coastal classes of 'Rocky', 'Gravel', 'Sand' and 'Man-made' (British Columbia Marine Conservation Analysis Project Team, 2011). Tidal current strength data (Foreman 1978) were quantified using root mean square (RMS) of tidal speeds modeled over a number of tidal cycles, and are used as an indication of relative current speed. RMS analysis is used to indicate relative mixing within estuaries and enclosed areas such as fjords and narrows (Etherington et al. 2007). Mixing is then used as an indicator of relative temperature and stratification conditions, where areas of

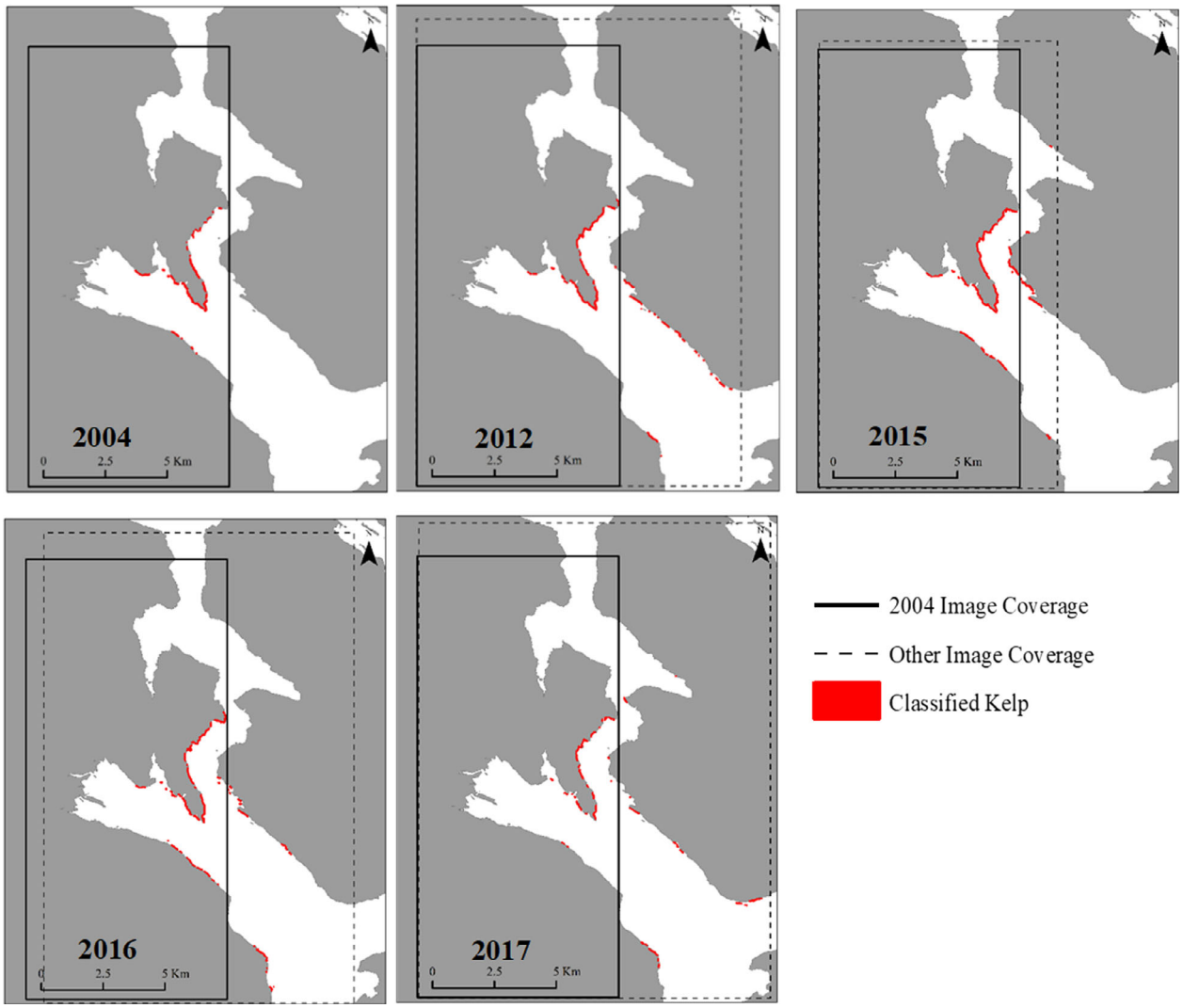

Figure 5. Classification results for the five images with each year's image extent shown in dashed lines. Note the difference in coverage area for the 2004 image which did not cover East Sansum.

high mixing indicate weak or no stratification, and therefore lower ocean temperature.

Multiple sources of sea surface temperature were considered including satellite-derived SST anomalies for the Strait of Georgia from 2003 to 2016 (Suchy et al. 2019) and SST data collected by a citizen science program as part of the Pacific Salmon Foundation's Salish Sea Marine Survival Project using CTD profiles collected in Cowichan Bay and Sansum Narrows from 2015 to 2017. The satellite-based data provide a broad scale picture of SST anomalies which may have been modified to varying degrees across the subregions due to local scale driver such as mixing and river effluent. The limited time series of local scale data from the citizen science program corroborates this effect, as temperatures measured in the narrows were 1-3 degrees lower than the satellite data.

Results

Image reliability

All images used for the persistence analysis showed high values for the reliability matrix, which were considered sufficient to detect the presence or absence of kelp within a 100 m shoreline unit. The kelp maps (Fig. 5) show similar patterns of kelp growth across years within the study areas. Specifically, the reliability matrix (Table 1) shows that the 2015 image exhibited the highest reliability (12)

Table 3. Validation error matrix for the 2016 Image using a subset of concurrent field data.

	Field data				
	Kelp	Non-kelp	Total	User accuracy	Total accuracy
Classification					
Kelp	376	83	459	81.9	86.9
Non-kelp	28	362	390	92.8	
Total	404	445	849		
Producer accuracy	93.1	81.4			

and the highest percentage of kelp (89.2%). The 2012 image had the lowest reliability (9) due to slightly poor environmental conditions, including tide height, glint and water surface roughness (Table 1). The lowest kelp presence was detected in 2017 (45.7%), which had the second highest reliability (11) (Table 1).

Classification

The results of the accuracy assessment for the 2016 image with concurrent field data yielded total (86.9%), users' (81.9%) and producers' (93.1%) accuracies (Table 3). The largest errors occurred in areas where kelp corresponded to single bulbs or small clusters. These errors were a result of the greater proportion of water in these pixels dampening the high NIR reflectance of kelp. Similar results, with accuracies between 74 and 94%, were reported in other studies using satellite imagery to map floating algae where high-density beds had higher accuracy (Fyfe et al. 1999; Casal et al. 2011).

For the remaining image years of 2004, 2012, 2015 and 2017, the analysis of distribution and median values for kelp NDVI and GNDVI for all image samples are described in a boxplot in Figure 4. The Wilcoxon signed-rank test shows that kelp NDVI values were the same as the 2016 reference pixels for all image years except 2004 and 2012, while the kelp GNDVI values were the same for all image years except 2012 (Table 4). The distribution of slightly higher NDVI and GNDVI values for 2004 and 2012 images are likely due to the presence of denser kelp beds than were present in the 2016 reference image rather than misclassification as spatial filtering and visual error adjustment would have removed any erroneous high NIR reflectance sources, such as glint or boats.

Spatial patterns of persistence

448 units were analyzed, representing 48.8 km of coastline (Figs. 6 and 7). Of the 448 units, 37.1% (166 units) had kelp present in at least 1 year (persistence > 0%). The regions north of Sansum Point (N, MB, OP), accounting for 31.2% (140) of all units, had kelp absent in all considered years (persistence = 0%). On the north side of Cowichan Bay (NC) and west side of Sansum Narrows (WS), persistence was generally high with 61.0% of units showing kelp present in at least 1 year. Specifically, in the WS region, 36.7% of shoreline units showed kelp present in all years and 54.4% in four or more years. In North Cowichan (NC), temporal presence of kelp was lower with 13.9% of units showing kelp in all years and 32.9% of units in four or more years, followed by even lower persistence measured on the south side of Cowichan Bay (SC), with no units having kelp in all years. The east side of Sansum Narrows (ES) also showed high persistence of kelp considering the four image years (excluding the 2004 image due to differences in image extents); kelp was present in about half of the 88 units and 50.0% of those kelp units had kelp present in at least 3 years.

Temporal change

To understand change over time in kelp presence, the 166-shoreline units (37.1% of the total number of units), which showed kelp present in at least 1 year, referred to as 'kelp units', were used in the analysis. The kelp units were used with the understanding that units where persistence = 0 do not have suitable environmental conditions for kelp to grow and no change will have occurred over time.

We then used this set of kelp units (166) to calculate the yearly percentage of units with kelp present. Regionally, the highest kelp presence was in 2015 (89.2%),

Table 4. Wilcoxon tests for differences between field data from 2016 base image and other imagery.

	NDVI			GNDVI		
Image year	W stat	*P* value	Difference	W stat	*P* value	Difference
2004	11902	<0.001	Yes	23901	0.0897	No
2012	15656	<0.001	Yes	12028	<0.0	Yes
2015	47028	0.988	No	48326	0.6571	No
2016	31482	0.1384	No	30384	0.1867	No
2017	24104	0.1029	No	24528	0.1683	No

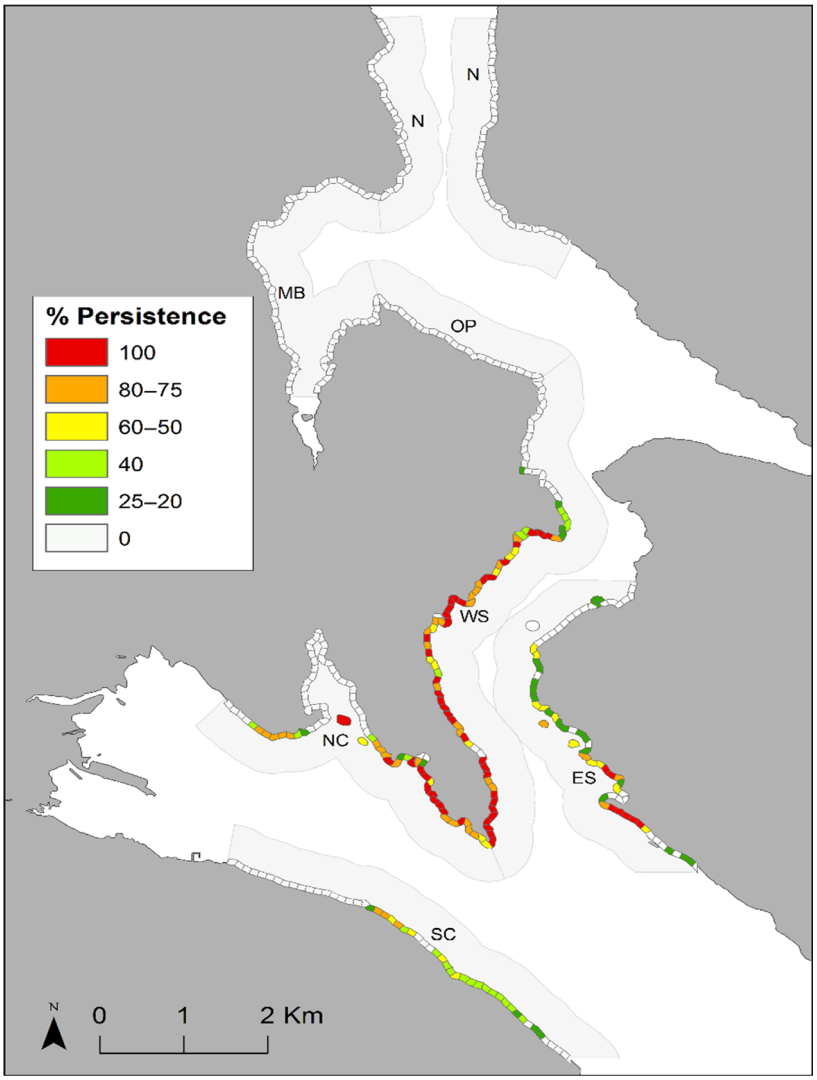

Figure 6. Persistence of kelp beds in Cowichan Bay and Sansum Narrows from 2004 to 2017. Shaded grey areas indicate the Sub regions of SC = South Cowichan, NC = North Cowichan, WS = West Sansum, ES = East Sansum, OP = Octopus point, MB = Maple Bay, N = North channel.

followed by 2016 (76.5%), 2004 (66.1%), 2012 (62.7%) and the lowest number was in 2017 (45.7%) (Fig. 8). This indicates that there was an overall decrease in kelp presence from 2015 to 2017 of 48.6%, with a general increase from 2012 to 2015 of 42.9%. Similar trends are seen on a sub-regional scale, where all sub-regions experienced a loss of kelp from 2015 to 2017. However, this was least pronounced in West Sansum where the decrease was 20.3% compared to the greatest decrease in South Cowichan of 86.4% (Fig. 8).

Spatial drivers

Figure 9 shows the greatest persistence of kelp when the substrate is rocky and where RMS tide is either low, 0.1, or medium between 0.3 and 0.6, on a scale of 0–1 (Foreman 1978). Figure 10 shows how East and West Sansum have both high proportions of rocky substrate and high RMS tide (>50% of area with values >0.5) and at the same time medium to high kelp persistence (Fig. 7), while areas which had low kelp persistence in Maple Bay, Octopus Point and North region (Fig. 7) had low RMS tide (values <0.3).

Discussion

Limitations of satellite imagery

In a satellite imagery-based method, using kelp presence or absence within a shoreline unit helps to reduce the likelihood that no kelp is detected due to beds that are too small or sparse in relation to the imagery spatial resolution. Still, it is possible that only small patches of kelp are present in a given shoreline unit and thus not detected in which case the unit will be recorded as having no kelp.

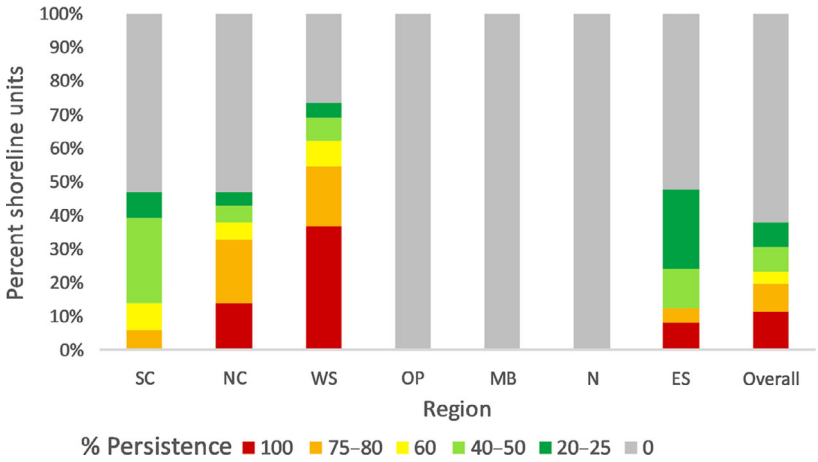

Figure 7. Percentage of total shoreline units with persistence of kelp by sub-region and entire region. East Sansum units are calculated from only four images (2012, 2015, 2016, and 2017) due to differences in number of images. For region definitions, see Figure 6.

Furthermore, the limited spatial and temporal extent of the dataset creates uncertainty in determining the drivers of kelp persistence. A longer time series of data with greater regional coverage would allow better understanding of variability and its relationships to long- and short-term local and global scale environmental conditions.

Other satellite platforms can be used for mapping kelp extent, each with their own strengths and weaknesses (Bennion et al. 2019; Schroeder et al. 2019). The use of commercial high-resolution satellite imagery as in this study allows the user to acquire images during optimal conditions of tide height, cloud cover, water conditions and kelp growth resulting in the highest quality imagery for mapping kelp. The high resolution allows small or fringing beds which are adjacent to the shoreline to be detected and may also be used to differentiate species (Botha et al. 2013) and estimate biomass (Andréfouët et al. 2004; Knudby and Nordlund 2011). However, commercial platforms may be cost prohibitive as tasking imagery can cost up to 30 USD/m^2 (DigitalGlobe.com. 2019). However, free sources of imagery such as from the Landsat series with a 30 m resolution much of the nearshore beds will be missed due to spectral mixing of pixels with land. Landsat is still a valuable source of imagery for mapping large kelp beds on a large scale where the use of an extensive historical time series can form composites of kelp extent seasonally and detect trends in kelp abundance and be averages to account for areas covered by cloud and differences in tide (Bell et al. 2018; Nijland et al. 2019). However, its application is limited to regions with large offshore beds of kelp (Nijland et al. 2019). Copernicus' Sentinel-2 is also a free source of imagery and with a spatial resolution of 10 m it may be more appropriate for monitoring fringing kelp moving forward as the mission began in 2015. Additionally, free open source software such as Google's Earth Engine and QGIS are making the use of satellite imagery for environmental monitoring increasingly accessible to a wider user base and allow for the automated analysis of imagery for use in broad scale mapping and change analysis (Nijland et al. 2019; Traganos et al. 2018. These broad scale maps can then be used to inform the selection of representative or important sites for more rigorous surveys.

Spatial drivers

The regions that had the highest kelp persistence were East and West Sansum (Figs. 6 and 7). These areas provide optimal growth conditions in regard to substrate type (rocky) and relatively strong currents a result of the narrow passage (~0.5 to 1.0 km) in Sansum Narrows (Mullan 2017). These stronger currents result in higher mixing and reduced stratification, which lead to lower temperature to which kelp is exposed compared to more stratified waters of Cowichan Bay.

The kelp persistence in Cowichan Bay may also be driven by substrate type and current strength. On the north side of Cowichan Bay there is a prevalence of rocky substrate, so despite the low currents recorded here (expressed as 0.1 RMS) kelp growth is supported (Figure 7 and 10). The lower persistence of kelp along the south side of Cowichan Bay is likely associated with substrate availability; here substrate consists of sand and gravel combined with lower currents, which allow for sediment deposition and less available substrate for kelp growth. Gravel and sand habitats typically indicate lower energy environments and favor species such as eelgrass, which attaches to substrate using root-like rhizomes (Mumford 2007). Limited availability of hard rocky substrate will constrain the amount of kelp that can grow and the presence of sandy substrate indicates deposition of sediment, which can smother kelp recruits.

The sub-regions north of Sansum Point (Octopus Point, Maple Bay and the North Channel) have similar

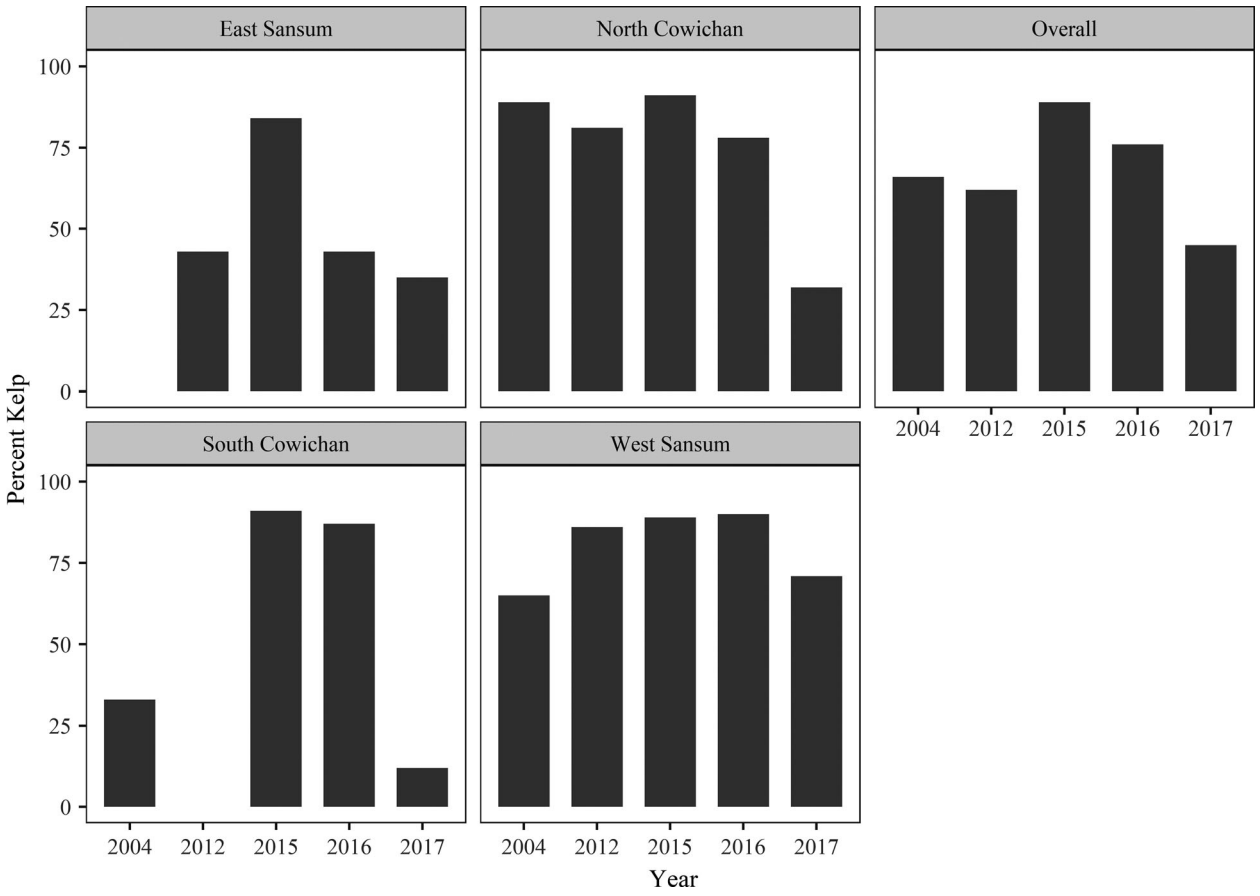

Figure 8. Percent of Kelp Units containing kelp each year by sub region and overall. Sub regions are: East Sansum (ES), North Cowichan (NC), South Cowichan (SC), and West Sansum (WS). Note OP, MB and N were not included as no units had kelp in any year. No data were available for ES in 2004 due to imagery coverage.

predominantly rocky substrate types and current regimes (>0.3) to North Cowichan; however, kelp is absent in these regions whereas there are persistent beds in North Cowichan. Conditions north of Sansum Point may be less optimal for kelp growth due to warmer SST and higher turbidity when compared with North Cowichan. These regions may experience a stronger influence from warmer, turbid, stratified waters from the Fraser River (Suchy et al. 2019).

Temporal changes

The general detected change in kelp presence may represent a true decline from 2015 to 2017 or it may be within the natural bounds of variation given that presence in 2015 (62.6%) was not much higher than in 2017 (45.7%). However, on a sub-regional scale, it appears there are large variations in kelp, especially in South Cowichan; here we observed 91.9% in 2015 and 12.5% in 2017. In nearby Washington State, Pfister et al. (2018) showed that there was little significant change in kelp persistence over a period from 1911 to 2015, except for areas in close proximity to human populations where kelp populations showed declines. Furthermore, Krumhansl et al. (2016) found a slight increasing trend in the Ecoregion containing Oregon, Washington, and Vancouver Island in studies spanning from 1983 to 2012, and suggested that local drivers including successful management practices, recovery of urchin predators and reduction in pollution are responsible for the differences from globally decreasing trends.

In the study area of Cowichan Bay and Sansum Narrows, environmental management has focused on the river and estuarine system including improving river levels, salt marsh and eelgrass bed restoration in support of creating habitat for juvenile salmon (https://www.cowichanestuary.com/projects-2/). More broadly, the provincial government has conducted limited inventories of coastal kelp resources for determining harvest quotas with the most recent in 2007 (Sutherland et al. 2008); however,

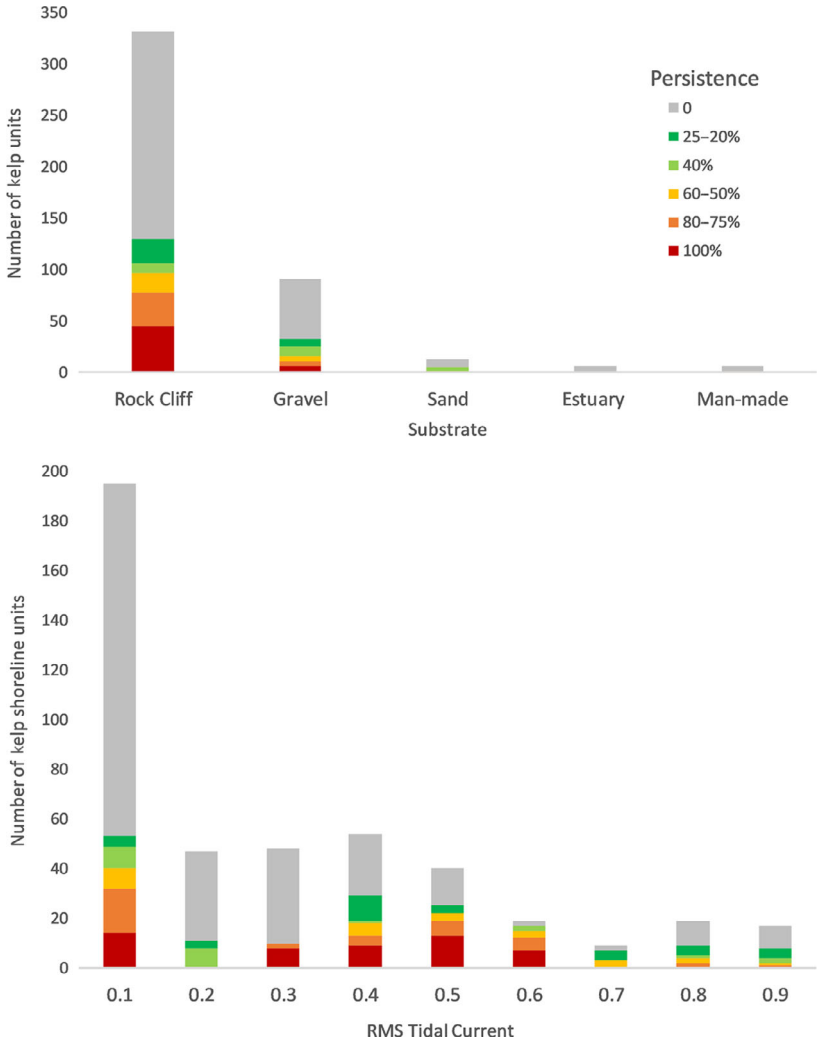

Figure 9. Kelp persistence across substrate types (top) and RMS tide (bottom), where RMS 0.1 is low current and 0.9 is high current.

kelp in the study is not harvested and the observed changes are likely associated with local environmental conditions.

The changes in persistence for the study region do not follow the expected trend in relation to large-scale climate indices. For instance, decreased kelp presence may occur during warm periods of the Pacific Decadal Oscillation (PDO) and El Nino Southern Oscillation (ENSO) as observed in Pfister et al. (2018) and higher kelp presence during positive phases of the North Pacific Gyre Oscillation (NPGO) when salinity and nutrients are high (Di Lorenzo et al. 2008). Instead, for 2015, the year with the highest recorded regional temperature anomalies during a positive PDO, our data showed the highest presence of kelp. In Washington State, the PDO, NPGO, and ENSO indices were found to have significant correlations with kelp abundance (Pfister et al. 2018), whereas lower temperatures (negative PDO, ENSO, positive NPGO) were associated with higher nutrients and increased kelp abundance (Bennion et al. 2019). Multiple studies have shown the inverse relationship between warm climate regimes and kelp abundance (Foreman 1984; Cavanaugh et al. 2011; Filbee-Dexter et al. 2016; Krumhansl et al. 2016; Pfister et al. 2018); however, the impacts may be short-lived given a switch to colder, nutrient rich conditions, which can provide opportunities for kelp to recover relatively quickly (Pfister et al. 2018).

Several factors may explain the changes in kelp persistence described in this study. Poor environmental conditions such as the warm SSTs recorded from 2013 to 2016, may have had a lag in the effects on the persistence of kelp. In these conditions, prolonged periods of exposure to water temperatures greater than 17°C have been shown to reduce spore formation and germination success (Vadas 1972; Springer et al. 2007). The warmer than average regional SSTs in 2015 and 2016 (Suchy et al. 2019), may be responsible for the lower presence of kelp in the subsequent years (2016, 2017) through reducing

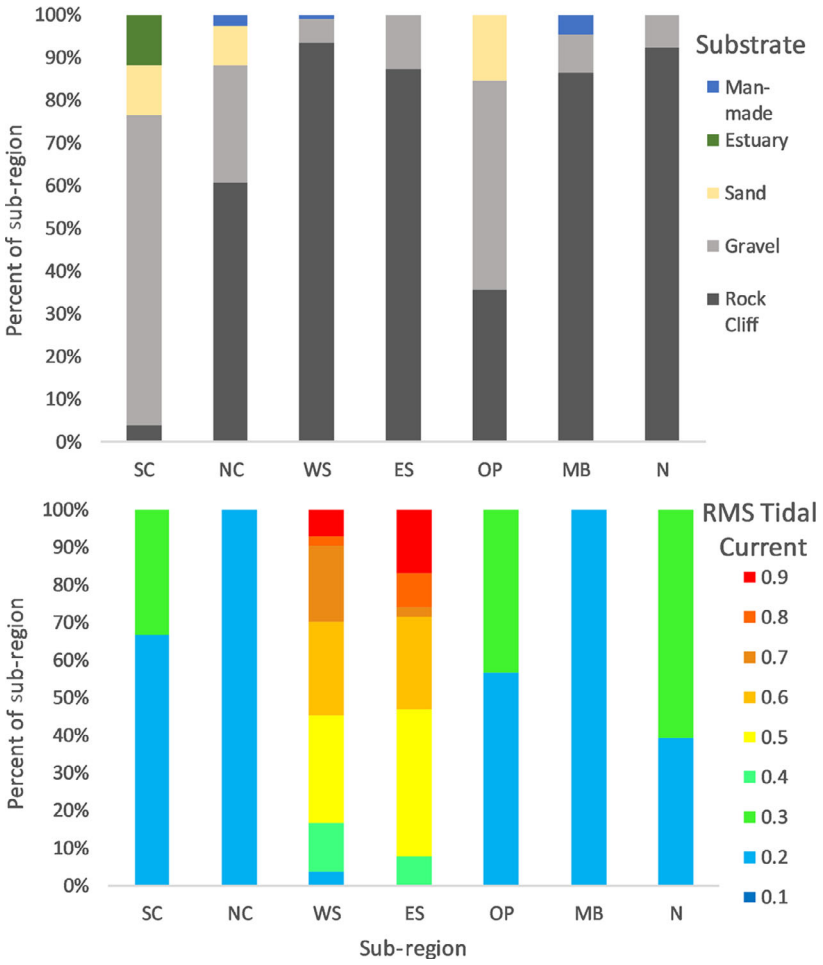

Figure 10. Coastal class (Top) and RMS tidal speeds (bottom) by Region. SC = South Cowichan, NC = North Cowichan, WS = West Sansum, ES = East Sansum, OP = Octopus Point, MB = Maple Bay, N = North.

spore production and germination (Dayton et al. 1998). Similarly, a 1-year lag was shown to be the best predictor of kelp growth and SST in Washington State (Pfister et al. 2018). Conversely, light availability, which also limits kelp growth, is more likely to cause within-year effects on kelp beds (Desmond et al. 2015). In 2015, positive anomalies in photosynthetic light availability were recorded for the Strait of Georgia region (Suchy et al. 2019), which may help to explain the high kelp presence for that year.

Furthermore, in situ measurements of SST from Cowichan Bay from 2015 to 2017 were on average 3°C cooler than those measured for the Strait of Georgia region, indicating that large-scale temperature anomalies were likely minimized due to the higher currents and stronger mixing in this sub-region. Because both nutrient availability and stratification are linked to temperature and mixing, this sub-region, particularly Sansum Narrows may experience better kelp growth conditions than the region as a whole. This is significant as the persistence of kelp populations here may be an important source of spores to adjacent areas and facilitate connectivity between habitats (Reed et al. 2004; Coleman et al. 2011; Olson et al. 2019).

Conclusion

Using high spatial resolution satellite imagery, temporal and spatial persistence of kelp was determined in the coastal waters of British Columbia. In this region, bull kelp showed higher persistence in areas with rocky substrate and well-mixed waters. Temporal analysis showed declines from 2015 to 2017, which may be due to local scale effects related to a lag effect from anomalous warm temperatures from 2015 to 2016.

The limitations of using satellite images for kelp detection include access to images with the appropriate spatial, spectral, temporal and physical coverage of the areas of interest, and the environmental conditions during acquisition such as tide height, season, sun glint and water surface. Using only images with the highest reliability, the resulting classifications show higher accuracy (86.9% in

relation to field surveys) and acceptable statistical performance compared to expected spectral characteristics of kelp for historical images.

Continuous and long-term mapping is needed to establish relationships between the measured persistence and environmental variables and to determine whether declines are long lasting or due to natural variability. By utilizing all available imagery sources such as new sensors like Sentinel-2 and developing automated processes for detecting kelp, a greater understanding of spatial and temporal drivers can be gained. Monitoring efforts may want to combine large scale mapping for broad scale spatial temporal distribution and use this data to select representative sites for yearly collection of more detailed data for validation of imagery and biological data. This will allow conservation and management initiatives to better understand and mitigate impacts to kelp ecosystems.

Acknowledgments

This research was funded by the Pacific Salmon Foundation as part of the Salish Sea Marine Survival Project (Publication number 38) with the University of Victoria. Fieldwork was conducted in partnership with Sea Change Marine Conservation Society and collaboration with the Mayne Island Conservancy, Pender Island Conservancy Association and Cowichan Tribes. Historical imagery was granted through the DigitalGlobe foundation.

Conflict of Interest

The authors have no conflicts of interest to declare.

References

Adler-Golden, S. M., W. W. Matthew, L. S. Bernstein, R. Y. Levine, A. Berk, S. C. Richtsmeier, et al. 1999. Atmospheric correction for shortwave spectral imagery based on MODTRAN4. *Imaging Spectrom.* **V 3753**, 61–69.

Airamé, S., J. E. Dugan, K. D. Lafferty, H. Leslie, D. A. McArdle, and R. R. Warner. 2003. Applying ecological criteria to marine reserve design: a case study from the California Channel Islands. *Ecol. Appl.* **13**, 170–184.

Andréfouët, S., M. Zubia, and C. Payri. 2004. Mapping and biomass estimation of the invasive brown algae *Turbinaria ornata* (Turner) J. Agardh and *Sargassum mangarevense* (Grunow) Setchell on heterogeneous Tahitian coral reefs using 4-meter resolution IKONOS satellite data. *Coral Reefs* **23**, 26–38.

Bao, N., A. M. Lechner, A. Fletcher, D. Mulligan, A. Mellor, and Z. Bai. 2012. Comparison of relative radiometric normalization methods using pseudo-invariant features for change detection studies in rural and urban landscapes. *J. Appl. Remote Sens.* **6**, 063578-1.

Bell, T. W., J. G. Allen, K. C. Cavanaugh, and D. A. Siegel. 2018. Three decades of variability in California's giant kelp forests from the Landsat satellites. *Remote Sens. Environ.*, 110811, in press. https://doi.org/10.1016/j.rse.2018.06.039

Bennion, M., J. Fisher, C. Yesson, and J. Brodie. 2019. Remote sensing of Kelp (*Laminariales, Ochrophyta*): monitoring tools and implications for wild harvesting. *Rev. Fish. Sci. Aquac.* **27**, 127–141. https://doi.org/10.1080/23308249.2018.1509056

Botha, E. J., V. E. Brando, J. M. Anstee, A. G. Dekker, and S. Sagar. 2013. Increased spectral resolution enhances coral detection under varying water conditions. *Remote Sens. Environ.* **131**, 247–261.

British Columbia Marine Conservation Analysis Project Team. 2011. Marine atlas of Pacific Canada: a product of the British Columbia marine conservation analysis. Available at: https://bcmca.ca/.

Britton-Simmons, K., J. E. Eckman, and D. O. Duggins. 2008. Effect of tidal currents and tidal stage on estimates of bed size in the kelp Nereocystis luetkeana. *Mar. Ecol. Prog. Ser.* **355**, 95–105.

Burt, J. M., M. T. Tinker, D. K. Okamoto, K. W. Demes, K. Holmes, and A. K. Salomon. 2018. Sudden collapse of a mesopredator reveals its complementary role in mediating rocky reef regime shifts. *Proc. R. Soc. B Biol. Sci.* **285**, 20180553.

California Department of Fish and Wildlife. 2016. "Perfect Storm" decimates Northern California kelp forests. 1. Available at:https://cdfwmarine.wordpress.com/2016/03/30/perfect-storm-decimates-kelp/. (Accessed: 25th June 2019)

Carney, L. T. 2005. Restoration of the bull kelp *Nereocystis luetkeana*. *Mar. Ecol. Prog. Ser.* **302**, 49–61.

Casal, G., N. Sánchez-Carnero, E. Sánchez-Rodríguez, and J. Freire. 2011. Remote sensing with SPOT-4 for mapping kelp forests in turbid waters on the South European Atlantic shelf. *Estuar. Coast. Shelf Sci.* **91**, 371–378.

Cavanaugh, K. C., D. A. Siegel, B. P. Kinlan, and D. C. Reed. 2010. Scaling giant kelp field measurements to regional scales using satellite observations. *Mar. Ecol. Prog. Ser.* **403**, 13–27.

Cavanaugh, K. C., D. A. Siegel, D. C. Reed, and P. E. Dennison. 2011. Environmental controls of giant-kelp biomass in the Santa Barbara Channel, California. *Mar. Ecol. Prog. Ser.* **429**, 1–17.

Chappell, R., and R. Pawlowicz. 2018. Atlas of oceanographic conditions in the strait of Georgia (2015-2017) based on the Pacific salmon foundation citizen science dataset. Department of Earth, Ocean and Atmoshperic Sciences, University of British Columbia.

Christie, H., K. M. Norderhaug, and S. Fredriksen. 2009. Macrophytes as habitat for fauna. *Mar. Ecol. Prog. Ser.* **396**, 221–233.

Claisse, J. T., D. J. Pondella, J. P. Williams, and J. Sadd. 2012. Using GIS mapping of the extent of nearshore rocky reefs to

estimate the abundance and reproductive output of important fishery species. *PLoS One* **7**, e30290.

Coleman, M. A., J. Chambers, N. A. Knott, H. A. Malcolm, D. Harasti, and A. Jordan. 2011. Connectivity within and among a network of temperate marine reserves. *PLoS One* **6**, e20168.

Dayton, P. K., M. J. Tegner, P. B. Edwards, and K. L. Riser. 1998. Sliding baselines, ghosts, and reduced expectations in kelp forest communities. *Ecol. Appl.* **8**, 309–322.

Desmond, M. J., D. W. Pritchard, and C. D. Hepburn. 2015. Light limitation within southern New Zealand kelp forest communities. *PLoS One* **10**, 1–18.

Deysher, L. E. 1993. Evaluation of remote sensing techniques for monitoring giant kelp populations. *Hydrobiologia* **260**, 307–312.

Di Lorenzo, E., N. Schneider, K. M. Cobb, P. J. S. Franks, K. Chhak, A. J. Miller, et al. 2008. North Pacific Gyre Oscillation links ocean climate and ecosystem change. *Geophys. Res. Lett.* **35**, 6.

DigitalGlobe.com. 2019. Available at:https://www.digitalglobe.com/. (Accessed: 2nd October 2019)

Druehl, L. D. 1968. Taxonomy and distribution of northeast pacific species of Laminaria. *Can. J. Bot.* **46**, 539–547.

Duarte, C. M., I. J. Losada, I. E. Hendriks, I. Mazarrasa, and N. Marbà. 2013. The role of coastal plant communities for climate change mitigation and adaptation. *Nat. Clim. Chang.* **3**, 961–968.

Duggins, D. O. 1980. Kelp beds and sea otters: an experimental approach. *Ecology* **61**, 447–453.

Estes, J. A., D. O. Duggins, and G. B. Rathbun. 1989. The ecology of extinctions in kelp forest communities. *Conserv. Biol.* **3**, 252–264.

Etherington, L. L., P. N. Hooge, E. R. Hooge, and D. F. Hill. 2007. Oceanography of Glacier Bay, Alaska: implications for biological patterns in a glacial fjord estuary. *Estuaries Coasts* **30**, 927–944.

Filbee-Dexter, K., and T. Wernberg. 2018. Rise of turfs: a new battlefront for globally declining kelp forests. *Bioscience* **68**, 64–76.

Filbee-Dexter, K., C. J. Feehan, and R. E. Scheibling. 2016. Large-scale degradation of a kelp ecosystem in an ocean warming hotspot. *Mar. Ecol. Prog. Ser.* **543**, 141–152.

Foreman, M. G. 1978. Manual for tidal currents analysis and prediction. Revised 2004. Pacific Mar. Sci. Rep. 78-6 57 pp.

Foreman, R. E. 1984. Studies on nereocystis growth in British Columbia, Canada. *Hydrobiologia* **116–117**, 325–332.

Foster, M. S., and D. R. Schiel. 2010. Loss of predators and the collapse of southern California kelp forests (?): alternatives, explanations and generalizations. *J. Exp. Mar. Bio. Ecol.* **393**, 59–70.

Fretwell, C., and L. Boyer. 2010. Guidelines and methods for mapping and monitoring kelp forest habitat in British Columbia. Guidelines and methods for mapping and monitoring kelp forest habitat in BC. Mayne island conservancy society, Seagrass Conservation Working Group. Pp. 1– 13. Available at:https://seachangesociety.com/wp-content/uploads/2015/10/Kelp-Monitoring-Methods.pdf.

Fyfe, J., S. A. Israel, A. Chong, N. Ismail, C. L. Hurd, K. Probert, et al. 1999. Mapping marine habitats in Otago, Southern New Zealand. *Geocarto Int.* **14**, 17–28.

Goldberg, S., J. Kirby, and S Licht. 2016. Applications of aerial multi-spectral imagery for algal bloom monitoring in rhode Island. SURFO Technical Report No. 16-01.http://digitalcommons.uri.edu/surfo_tech_reports/13.

Gupta, R. P., T. K. Reet, V. Saini, and N. Srivastava. 2013. A simplified approach for interpreting principal component images. *Adv. Remote Sens.* **2**, 111–119.

Halpern, B. S., K. Cottenie, and B. R. Broitman. 2006. Strong top-down control in Southern California kelp forest ecosystems. *Science* **312**, 1230–1232.

Hernández, C. A., C. Sangil, A. Fanai, and J. C. Hernández. 2018. Macroalgal response to a warmer ocean with higher CO2 concentration. *Mar. Environ. Res.* **136**, 99–105.

Knudby, A., and L. Nordlund. 2011. Remote sensing of seagrasses in a patchy multi-species environment. *Int. J. Remote Sens.* **32**, 2227–2244.

Krumhansl, K. A., and R. E. Scheibling. 2012. Production and fate of kelp detritus. *Mar. Ecol. Prog. Ser.* **467**, 281–302

Krumhansl, K. A., D. K. Okamoto, A. Rassweiler, M. Novak, J. J. Bolton, K. C. Cavanaugh, et al. 2016. Global patterns of kelp forest change over the past half-century. *Proc. Natl. Acad. Sci. USA* **113**, 13785–13790.

Lorentsen, S. H., K. Sjøtun, and D. Grémillet. 2010. Multi-trophic consequences of kelp harvest. *Biol. Conserv.* **143**, 2054–2062.

Mullan, S. 2017. Tidal sedimentology and geomorphology in the central Salish Sea straits, British Columbia and Washington State. (PhD Thesis). (University of Victoria, Canada, 2017).

Mumford, T. F. 2007. Kelp and eelgrass in puget sound. Puget sound nearshore partnership report No. 2007-05.

Nahirnick, N. K., L. Reshitnyk, M. Campbell, M. Hessing-Lewis, M. Costa, J. Yakimishyn, et al. 2019. Mapping with confidence; delineating seagrass habitats using Unoccupied Aerial Systems (UAS). *Remote Sens. Ecol. Conserv.* **5**, 121–135.

Nijland, W., L. Reshitnyk, and E. Rubidge. 2019. Satellite remote sensing of canopy-forming kelp on a complex coastline: a novel procedure using the Landsat image archive. *Remote Sens. Environ.* **220**, 41–50.

Olson, A. M., M. Hessing-Lewis, D. Haggarty, and F. Juanes. 2019. Nearshore seascape connectivity enhances seagrass meadow nursery function. *Ecol. Appl.* **29**, 275–284.

Padma, S., and S. Sanjeevi. 2014. Jeffries Matusita based mixed-measure for improved spectral matching in hyperspectral image analysis. *Int. J. Appl. Earth Obs. Geoinf.* **32**, 138–151.

Peterson, C. H., S. D. Rice, J. W. Short, D. Esler, J. L. Bodkin, B. E. Ballachey, et al. 2003. Long-term ecosystem response to the exxon valdez oil spill. *Science* **302**, 2082–2086.

Pfister, C. A., H. D. Berry, and T. Mumford. 2018. The dynamics of Kelp Forests in the Northeast Pacific Ocean and the relationship with environmental drivers. *J. Ecol.* **46**, 1–14.https://doi.org/10.1111/1365-2745.12908.

Reed, D. C., S. C. Schroeter, and P. T. Raimondi. 2004. Spore supply and habitat availability as sources of recruitment limitation in the giant kelp *Macrocystis pyrifera* (Phaeophyceae). *J. Phycol.* **40**, 275–284.

Reed, D. C., A. Rassweiler, M. H. Carr, K. C. Cavanaugh, D. P. Malone, and D. A. Siegel. 2011. Wave disturbance overwhelms top-down and bottom-up control of primary production in California kelp forests. *Ecology* **92**, 2108–2116.

Rouse, J., R. Haas, J. Schell, and D. Deering. 1974. Monitoring vegetation systems in the Great Plains with ERTS. Pp. 309–317 in *Third ERTS Symposium, NASA SP-351*.https://doi.org/10.1002/mrm.26868

Schiel,D. R., J. R. Steinbeck, and M. S. Ten Foster. 2004. Years of induced ocean warming causes comprehensive changes in marine benthic communities. *Ecology* **85**, 1833–1839.

Schowengerdt, R. A. 2012. *Remote sensing models and methods for image processing*. Elsevier, Burlington, Massachusetts.

Schroeder, S. B., C. Dupont, L. Boyer, F. Juanes, and M. Costa. 2019. Passive remote sensing technology for mapping bull kelp (*Nereocystis luetkeana*): a review of techniques and regional case study. *Glob. Ecol. Conserv.* **19**, e00683.

Shaffer, A. 2004. Preferential use of nearshore kelp habitats by juvenile salmon and forage fish.

Shaffer, J. A., and D. S. Parks. 1994. Seasonal variations in and observations of landslide impacts on the algal composition of a puget sound nearshore kelp forest. *Bot. Mar.* **37**, 315–324.

Simonson, E. J., R. E. Scheibling, and A. Metaxas. 2015. Kelp in hot water: I. Warming seawater temperature induces weakening and loss of kelp tissue. *Mar. Ecol. Prog. Ser.* **537**, 89–104.

Springer, Y., C. Hays, M. Carr, and M. Mackey. 2007. Ecology and management of the bull kelp, (Nereocystis luetkeana): a synthesis with recommendations for future research. Lenfest Ocean Program, Washington, DC, USA. 48.

Stekoll, M. S., L. E. Deysher, and M. Hess. 2006. A remote sensing approach to estimating harvestable kelp biomass. *J. Appl. Phycol.* **18**, 323–334.

Steneck, R. S., M. H. Graham, B. J. Bourque, D. Corbett, J. M. Erlandson, J. A. Estes, et al. 2002. Kelp forest ecosystems: biodiversity, stability, resilience and future. *Environ. Conserv.* **29**, 436–459.

Suchy, K., M. Costa, and I. Perry. 2019. Influence of environmental drivers on satellite-derived chlorophyll a in the Strait of Georgia. *Prog. Oceanogr.* **176**, 102134.

Sutherland, I. R., V. Karpouzi, M. Mamoser, and B. Carswell. 2008. Kelp Inventory, 2007: areas of the British Columbia central coast from Hakai passage to the Bardswell group. (Ministry of Environment, Oceans and Marine Fisheries Branch, 2008).

Taheri, S. M., and G. Hesamian. 2013. A generalization of the Wilcoxon signed-rank test and its applications. *Stat. Pap.* **54**, 457–470.

Taylor, D. I., and D. R. Schiel. 2005. Self-replacement and community modification by the southern bull kelp (*Durvillaea antarctica*). *Mar. Ecol. Prog. Ser.* **288**, 87–102.

Teagle, H., S. J. Hawkins, P. J. Moore, and D. A. Smale. 2017. The role of kelp species as biogenic habitat formers in coastal marine ecosystems. *J. Exp. Mar. Bio. Ecol.* **492**, 81–98.

Tou, J. T., and R. C. Gonzalez. 1974. *Pattern recognition principles*. Addison-Wesley Publishing Co, Reading, Massachusetts.

Traganos, D., B. Aggarwal, D. Poursanidis, K. Topouzelis, N. Chrysoulakis, P. Reinartz, et al. 2018. Towards global-scale seagrass mapping and monitoring using Sentinel-2 on Google Earth Engine: the case study of the Aegean and Ionian Seas. *Remote Sens.* **10**, 1–14.

Uhl, F., I. Bartsch, and N. Oppelt. 2016. Submerged kelp detection with hyperspectral data. *Remote Sens.* **8**, 487.

Vadas, R. L. 1972. Ecological implications of culture studies on nereocystis luetkeana. *J. Phycol.* **8**, 196–203.

Waldichuk, M. 1957. Physical oceanography of the strait of Georgia, British Columbia. *Fish. Res. Board Canada* **14**, 321–486.

Young, M., K. Cavanaugh, T. Bell, P. Raimondi, C. A. Edwards, P. T. Drake, et al. 2016. Environmental controls on spatial patterns in the long-term persistence of giant kelp. *Ecology* **86**, 45–60.

